Multicolor Čerenkov conical beams generation by cascaded-χ(2) processes in radially poled nonlinear photonic crystals

H. X. Li, S. Y. Mu, P. Xu, M. L. Zhong, C. D. Chen, X. P. Hu, W. N. Cui, and S. N. Zhu

Citation: Applied Physics Letters **100**, 101101 (2012); doi: 10.1063/1.3692593
View online: http://dx.doi.org/10.1063/1.3692593
View Table of Contents: http://scitation.aip.org/content/aip/journal/apl/100/10?ver=pdfcov
Published by the AIP Publishing

Multicolor Čerenkov conical beams generation by cascaded-$\chi^{(2)}$ processes in radially poled nonlinear photonic crystals

H. X. Li,[1,2] S. Y. Mu,[1] P. Xu,[1,a)] M. L. Zhong,[1] C. D. Chen,[1] X. P. Hu,[1] W. N. Cui,[2] and S. N. Zhu[1,a)]
[1]*National Laboratory of Solid State Microstructures and School of Physics, Nanjing University, Nanjing 210093, People's Republic of China*
[2]*Department of Applied Physics, Nanjing University of Science and Technology, Nanjing 210094, People's Republic of China*

(Received 11 January 2012; accepted 20 February 2012; published online 5 March 2012)

We observe multiple simultaneous cascaded-$\chi^{(2)}$ Čerenkov conical radiations in radially poled nonlinear photonic crystals. By using two incident fundamental waves ω_1 and ω_2, a variety of cascaded nonlinear up-conversion processes occur which result in high-frequency Čerenkov radiations at $2\omega_i + \omega_j (i, j = 1, 2)$ exhibiting as multicolor conical beams. Two types of phase-matching geometries with different emission angles are demonstrated for each kind of cascaded-$\chi^{(2)}$ Čerenkov radiation. The external angle of the Čerenkov radiation exhibits strong dependence on the fundamental wavelengths. The experimental results agree well with the theoretical calculations.
 [http://dx.doi.org/10.1063/1.3692593]

Conical optical beams have attracted great interest in recent years due to their wide potential applications in light manipulation,[1–3] nonlinear conversion efficiency enhancement,[4] domain structure diagnosis,[5–7] *in vivo* mouse imaging reconstruction,[8] and entangled photon pairs generation.[9–11] Nonlinear optical processes,[5,6] especially nonlinear Čerenkov conical radiations,[12–14] are superior in generating conical beams, where the beam front is shaped by phase-matching conditions. Similar to Čerenkov radiation of charged particles, the nonlinear Čerenkov radiation is also observable at a conical wave front defined by the cone angle $\theta_c = \arccos(v'/v)$, where v' and v are the phase velocities of the radiation wave and the nonlinear polarization under $v > v'$.[15] The Čerenkov-type parametric processes are highly enhanced due to the existence of the domain walls and to the modulation of $\chi^{(2)}$ in nonlinear photonic crystals. It had even been observed in an extreme case where a single boundary between two inversely oriented ferroelectric domains was illuminated.[16] The radiation source for the nonlinear Čerenkov emission is a spatially extended collection of dipoles rather than a point particle in traditional electric Čerenkov radiation. Hence, any intense wave propagating in an optical medium may induce the Čerenkov-type nonlinear polarization. The Čerenkov second harmonic,[12–16] sum-frequency,[13] and difference-frequency generations in waveguides[17] had been investigated. Most of previous studies focus on single $\chi^{(2)}$ Čerenkov radiation except for the recent reports on the Čerenkov third harmonic generation (CTHG).[18–21] Herein, we investigate the more complex cascaded-$\chi^{(2)}$ nonlinear processes which result in high-frequency Čerenkov radiations. By employing two collinear incident fundamental beams, $\chi^{(2)}$ up-conversion processes such as second harmonic generation and sum-frequency generation may cascade, leading to simultaneous multi-frequency Čerenkov conical radiations. For each cascaded Čerenkov radiation, two types of phase-matching geometries are demonstrated.

A z-cut congruent $LiTaO_3$ crystal with a thickness of 0.5 mm was electrically poled to possess a radial pattern with an azimuthal angle of 0.3°. It has a smallest period of 2.1 μm, a duty cycle of 30%, and an outer/inner diameter of 3.0/1.2 mm. Figure 1(a) shows its schematic radial structure as well as the partial microscopic image of the surface-etched sample. It can be seen that the reversed domains are

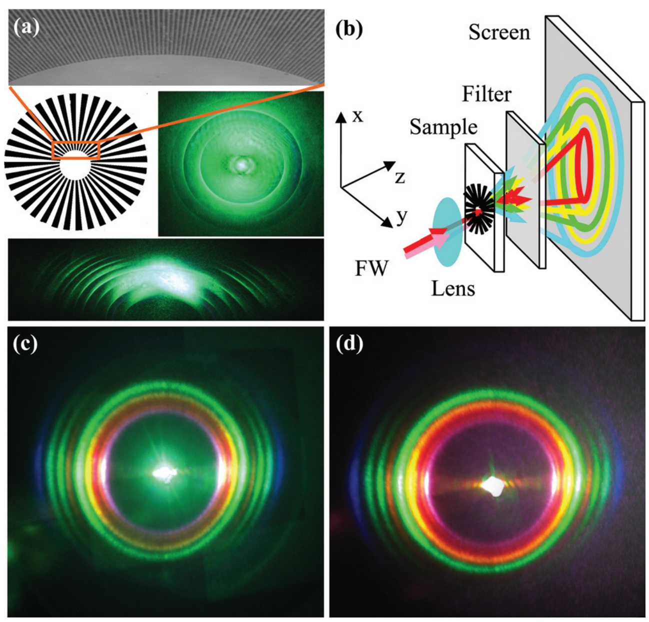

FIG. 1. (Color) (a) Schematic of the radially poled nonlinear photonic crystal ($LiTaO_3$) and the partial optical microscopic image of the sample with an azimuthal angle of 0.3° and a smallest poling period of 2.1 μm. The measured diffraction patterns of the central and edge parts of the radial structure for green incident light are also presented. (b) Schematic of the experimental setup with two fundamental waves propagating along the optic axis of the crystal. (c) and (d) Multiple rings of Čerenkov conical radiations for cases with two fundamental wavelengths (signal/idler) of 1474.1/1744.7 and 1456/1771 nm, respectively.

a)Authors to whom correspondence should be addressed. Electronic addresses: pingxu520@nju.edu.cn and zhusn@nju.edu.cn.

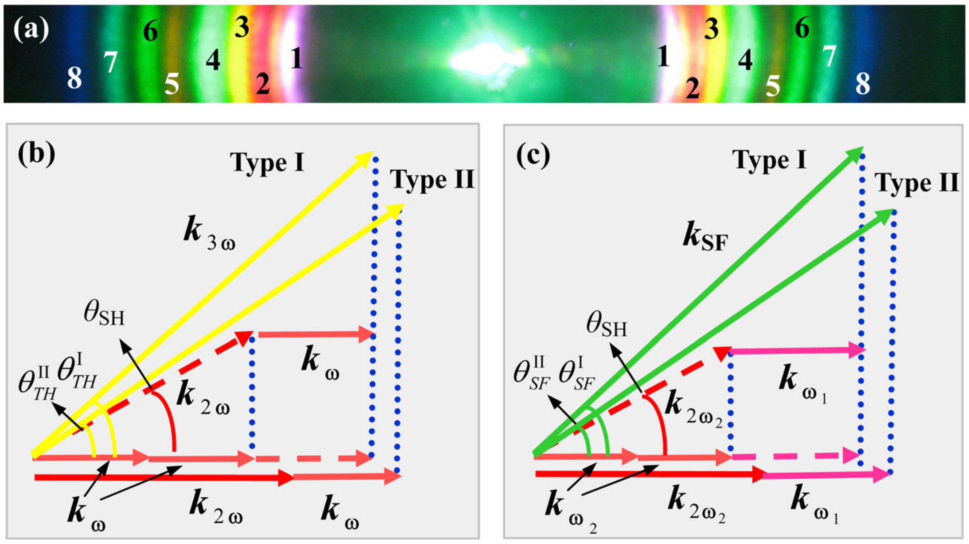

FIG. 2. (Color online) (a) Magnified central part of the image shown in Fig. 1(d). Numbers 1-8 refer to the radiated Čerenkov second harmonic generation, type I and type II third harmonic generations, and type I and type II cascaded sum-frequency generations (Table I), respectively. (b) and (c) The schematic diagram showing the phase-matching geometries of the Čerenkov third harmonic and sum-frequency generations.

uniform over the whole sample despite of its small poling period. Figure 1(a) also displays the diffraction pattern, i.e., the Fourier spectrum of the radial structure under illumination of green light. The pattern exhibits as rings for light incident onto the central region of the radial structure. The circular arc lines are observed for light incident on an area deviating from the central part. All the diffraction patterns were recorded far from the sample. The experimental setup was depicted in Fig. 1(b). A passively mode-locked femtosecond oscillator combined with an optical parametric amplifier generates the 800 nm pump (pulse width: 150 fs; repetition rate: 5 kHz). Two fundamental beams, signal (F1) and idler (F2), are down converted from the 800 nm pump, whose wavelengths can be tuned between 1.3-2.1 μm. They are perpendicularly polarized and propagate along the z-axis of the sample. A lens was used to loosely focus the beam, and the sample was placed off the focus plane. The beam waist of the fundamental waves on the surface of the crystal is around 180 μm. Figures 1(c) and 1(d) display the typical images of the multiple Čerenkov rings for the cases with fundamental wavelengths (F1/F2) of 1474.1/1744.7 nm and 1456/1771 nm, respectively. For the former case, the powers of the fundamental beams are 400/330 mW, while the total power intensity on the sample is 3.8 TW/cm^2. The magnified partial image of Fig. 1(c) is displayed in Fig. 2(a). The rings exhibit higher intensity for more inner incidence of the fundamental beams on the surface of the radially poled nonlinear photonic crystals. Considering that the more inner region of the crystal possesses greater overall area of domains walls, hence, this observation supports the conjecture that the domain walls of the nonlinear photonic crystals can highly enhance the Čerenkov radiation.

The measured values of the cone angles and the frequencies of the rings corresponding to fundamental wavelengths of 1474.1/1744.7 nm are shown in Table I. These Čerenkov conical beams can be identified as cascaded-$\chi^{(2)}$ or single-$\chi^{(2)}$ processes, respectively. The rings 1 and 2 are assigned to the second harmonic of the fundamental beams. The ring 1 is infrared and can only be identified through a digital camera. The external angles of rings 1 and 2 are 23.4° and 25.7°, respectively, well obeying the Čerenkov second harmonic relation $k_2 \cos\theta = 2k_1$. The calculated values of the external conical angles by using Snell's law[12] are also presented in Table I. This type of Čerenkov radiation had previously been studied.[12,13]

In the following sections, we shall model and explain the observed various cascaded-$\chi^{(2)}$ Čerenkov radiations. Successive second harmonic generation and sum-frequency generation will lead to high-frequency Čerenkov radiations at $2\omega_i + \omega_j (i, j = 1, 2)$, where ω_1 and ω_2 are the frequencies of the fundamental waves. The first kind of Čerenkov radiation is the Čerenkov third harmonic generation. The rings 3 and 5 (Fig. 2(a)) which possess radiation angles of 29.3° and 35.6° along with an identical wavelength of 582 nm are third harmonic of the idler fundamental wave (1744.7 nm). The ring 5 is so weak that it seemed to have different color with respect to ring 3 ascribed to color distortion of the CCD camera. Our theoretical calculation shows that there are two types of phase-matching geometries (Fig. 2(b)) for the Čerenkov third harmonic generation. Considering the small value of $\chi^{(3)}$ for the congruent $LiTaO_3$, the observed third

TABLE I. Experimental and calculated external radiate angles of Čerenkov rings[a].

Number	Wavelength (nm)	Type	Calculated angle (°)	Experimental angle (°)
1	863	SH of F2	23.7	23.4
2	737	SH of F1	25.5	25.7
5	582	Type I TH of F2	35.6	35.6
3	582	Type II TH of F2	29.6	29.3
8	491	Type I TH of F1	41.9	41.9
10	491	Type II TH of F1	35.4	-
6	548	Type I SF (SH2 + F1)	37.4	37.2
4	548	Type II SF (SH2 + F1)	31.9	32.2
7	517	Type I SF (SH1 + F2)	39.4	39.5
9	517	Type II SF (SH1 + F2)	32.5	…

[a]F1/F2 refers to the fundamental wave with wavelength of 1474.0/1744.7 nm, and SH1 (863 nm)/SH2 (737 nm) refers to the second harmonic of F1/F2, respectively.

harmonic generation (THG) should result from a two-step cascading process.[19–21] The first step involves the second harmonic generation (SHG) and the second involves the sum-frequency of the second harmonic and the fundamental wave. For the first SHG process, the harmonic beam may be collinear or noncollinear relative to the fundamental beam. The noncollinear SHG is a Čerenkov radiation, whose longitudinal component (along the z axis) of the wavevectors is conserved. The resulting Čerenkov THG is called type I CTHG (ring 5 for F2). The cascaded sum-frequency of the collinear SHG and the fundamental beam results in type II CTHG (ring 3 for F2). The collinear SHG generates at the high peak power of the femtosecond laser although the phase-matching condition is not strictly satisfied. The phase-matching conditions for these two types of Čerenkov THGs can be expressed as

$$k_{3\omega}\cos\theta^{\mathrm{I}}_{TH} = k_{2\omega}\cos\theta_{SH} + k_{\omega}, \tag{1}$$

$$k_{3\omega}\cos\theta^{\mathrm{II}}_{\mathrm{TH}} = k_{2\omega} + k_{\omega}, \tag{2}$$

where k_{ω}, $k_{2\omega}$, and $k_{3\omega}$ are wavevectors of the fundamental, second harmonic, and third harmonic beams; and θ_{SH}, θ^{I}_{TH}, and $\theta^{\mathrm{II}}_{\mathrm{TH}}$ represent the emission angles of the Čerenkov SHG, type I CTHG, and type II CTHG, respectively. Then, we have $\theta^{\mathrm{I}}_{TH} = \arccos(n_1/n_3)$ for type I CTHG and $\theta^{\mathrm{II}}_{\mathrm{TH}} = \arccos(\frac{2n_2+n_1}{3n_3})$ for type II CTHG, where n_1, n_2, and n_3 are the refraction indices of the fundamental, second harmonic, and third harmonic beams, respectively. It is easy to verify that $\theta^{\mathrm{II}}_{\mathrm{TH}} < \theta^{\mathrm{I}}_{TH}$. Measured values of θ^{I}_{TH} and $\theta^{\mathrm{II}}_{\mathrm{TH}}$ are 35.6° and 29.3°, respectively, which are in good agreement with theoretical ones. The type I CTHG had been observed recently.[20] The CTHG process for the signal was observed in our experiment too. Our theoretical calculation gives the values of the external conical angles of type I and type II CTHG of the signal light as 35.4° and 41.9°. In experiment, only the ring 8 with a conical angle of 41.9° for type I CTHG can be identified. The expected ring 10 with a conical angle of 35.4° for type II CTHG cannot be well identified because it is very weak due to phase-mismatching and that it is very close to the much brighter ring 5 (type I CTHG of idler). The ring 9 cannot be identified due to the same reason.

The second kind of cascaded-$\chi^{(2)}$ Čerenkov radiation is the generation of new frequencies at $2\omega_1 + \omega_2$ or $2\omega_2 + \omega_1$ from the combination of two fundamental beams. For each Čerenkov radiation frequency, there also exist two types of phase-matching geometries (Fig. 2(c)), i.e., the sum-frequency of the noncollinear or collinear SHG of one fundamental beam with another fundamental beam. The former is called type I cascade-$\chi^{(2)}$ Čerenkov sum-frequency generation (CSFG) and the latter type II CSFG. The corresponding phase-matching conditions are

$$k_{SF}\cos\theta^{\mathrm{I}}_{SF} = k_{2\omega_2}\cos\theta_{SH} + k_{\omega_1}, \tag{3}$$

$$k_{SF}\cos\theta^{\mathrm{II}}_{SF} = k_{2\omega_2} + k_{\omega_1}, \tag{4}$$

where k_{ω_1}, $k_{2\omega_2}$, and k_{SF} are the wavevectors of the fundamental wave ω_1, second harmonics of ω_2, and their sum-freqeuncy $2\omega_2 + \omega_1$; θ_{SH}, θ^{I}_{SF}, and $\theta^{\mathrm{II}}_{SF}$ are the external radiate angles of the Čerenkov SHG, type I CSFG, and type II CSFG, respectively. We, thus, can obtain

$$\theta^{\mathrm{I}}_{SF} = \arccos\left(\frac{2n_2\omega_2 + n_1\omega_1}{n_{SF}(2\omega_2 + \omega_1)}\right), \tag{5}$$

$$\theta^{\mathrm{II}}_{SF} = \arccos\left(\frac{2n_{2\omega_2}\omega_2 + n_1\omega_1}{n_{SF}(2\omega_2 + \omega_1)}\right), \tag{6}$$

where n_1, n_2, $n_{2\omega_2}$, and n_{SF} are the refraction indices of frequency ω_1, ω_2, $2\omega_2$, and $2\omega_2 + \omega_1$, respectively. It is easy to verify that $\theta^{\mathrm{II}}_{SF} < \theta^{\mathrm{I}}_{SF}$. The measured values of θ^{I}_{SF} and $\theta^{\mathrm{II}}_{SF}$ are 37.2° and 32.2°, respectively, in good agreement with calculated values (Table I). The rings 4 and 6 with an identical wavelength of 548 nm are assigned to the two types of CSFG. Note that the CSFG at $2\omega_1 + \omega_2$ shows similar behavior to those of CSFG at $2\omega_2 + \omega_1$. Our results show that some different Čerenkov nonlinear radiations, such as type II CSFG of $2\omega_1 + \omega_2$ and $2\omega_2 + \omega_1$, can have an identical external angle, thereby their rings overlap.

The external angles of the cascade-$\chi^{(2)}$ Čerenkov conical beams depend on the fundamental wavelengths. Figure 3 displays the measured values of the external angles of the Čerenkov CTHG and CSFG versus the fundamental wavelengths. It can be seen that all of the external angles decrease monotonically with increasing wavelength of signal. The external angle of type I CSFG changes only slightly with varying fundamental wavelengths.

We observe also the cascade-$\chi^{(2)}$ Čerenkov radiations in other types (one-dimensional periodically poled and two-

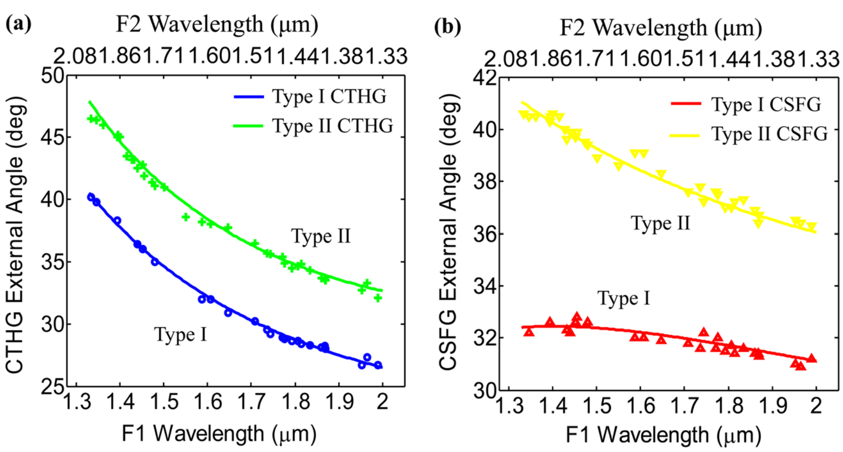

FIG. 3. (Color online) Plot of the experimental (signs) and calculated values (solid lines) of the external radiate angles of (a) Čerenkov third harmonic generation and (b) Čerenkov sum-frequency generation versus fundamental wavelengths (F1: signal; F2: idler).

dimensional hexgonally poled) of nonlinear photonic crystals. They exhibit different diffraction patterns with respect to those of the radially poled nonlinear photonic crystals, and there exists sixfold modulation of the azimuthal intensity distribution for them. Additionally, the difference between the refractive indices of the ordinary and extraordinary waves of $LiTaO_3$ is rather small, leading to almost overlapped rings for them; and as a result, the light of the rings generally occupy elliptical polarization at each azimuthal angle.[12,20]

In summary, we have studied the simultaneously arising colorful Čerenkov conical beams generated by cascade-$\chi^{(2)}$ processes in radially poled nonlinear photonic crystals. Two types of phase-matching geometries exist for each kind of cascade-$\chi^{(2)}$ Čerenkov radiation. These nonlinear responses of the nonlinear photonic crystals can be tuned over a very wide frequency range demonstrating their advantage in obtaining conical beams with different wavelengths and different emission angles. Therefore, they can find wide applications in many areas such as light manipulation and domain structure diagnosis.

This work was supported by the State Key Program for Basic Research of China (Nos. 2012CB921802 and 2011CBA00205) and the National Natural Science Foundations of China (Nos. 11104145, 91121001, and 11021403). It was also supported by the Priority Academic Program Development of Jiangsu Higher Education Institutions (PAPD).

[1]D. P. O'Dwyer, C. F. Phelan, K. E. Ballantine, Y. P. Rakovich, J. G. Lunney, and J. F. Donegan, Opt. Express **18**, 27319 (2010).
[2]J. P. Yin, W. J. Gao, and Y. F. Zhu, Prog. Opt. **45**, 119 (2003).
[3]J. Trull, S. Saltiel, V. Roppo, C. Cojocaru, D. Dumay, W. Krolikowski, D. N. Neshev, R. Vilaseca, K. Staliunas, and Y. S. Kivshar, Appl. Phys. B **95**, 609 (2009).
[4]B. Glushko, B. Kryzhanovsky, and D. Sarkisyan, Phys. Rev. Lett. **71**, 243 (2003).
[5]P. Xu, S. H. Ji, S. N. Zhu, X. Q. Yu, J. Sun, H. T. Wang, J. L. He, Y. Y. Zhu, and N. B. Ming, Phys. Rev. Lett. **93**, 133904 (2004).
[6]S. M. Saltiel, D. N. Neshev, W. Krolikowski, N. Voloch-Bloch, A. Arie, and Y. S. Kivshar, Phys. Rev. Lett. **104**, 083902 (2010).
[7]Y. Sheng, A. Best, R. Shiloh, H. Butt, W. Krolikowski, A. Arie, and K. Koynov, Opt. Express **18**, 16539 (2010).
[8]C. Q. Li, G. S. Mitchell, and S. R. Cherry, Opt. Lett. **35**, 1109 (2010).
[9]C. K. Hong, Z. Y. Ou, and L. Mandel, Phys. Rev. Lett. **59**, 2044 (1987).
[10]Y. H. Shih and C. O. Alley, Phys. Rev. Lett. **61**, 2921 (1988).
[11]M. N. Nasr, S. Carrasco, B. E. A. Saleh, A. V. Sergienko, M. C. Teich, J. P. Torres, L. Torner, D. S. Hum, and M. M. Fejer, Phys. Rev. Lett. **100**, 183601 (2008).
[12]S. M. Saltiel, Y. Sheng, N. Voloch-Bloch, D. N. Neshev, W. Krolikowski, A. Arie, K. Koynov, and Y. S. Kivshar, IEEE J. Quantum Electron. **45**, 1465 (2009).
[13]P. Molina, M. O. Ramirez, and L. E. Bausa, Adv. Funct. Mater. **18**, 709 (2008).
[14]W. J. Wang, Y. Sheng, Y. F. Kong, A. Arie, and W. Krolikowski, Opt. Lett. **35**, 3790 (2010).
[15]Y. Zhang, Z. D. Gao, Z. Qi, S. N. Zhu, and N. B. Ming, Phys. Rev. Lett. **100**, 163904 (2008).
[16]X. W. Deng and X. Chen, Opt. Express **18**, 15597 (2010).
[17]K. Suizu, K. Koketsu, T. Shibuya, T. Tsutsui, T. Akiba, and K. Kawase, Opt. Express **17**, 6676 (2009).
[18]W. Wang, V. Roppo, K. Kalinowski, Y. Kong, D. N. Neshev, C. Cojocaru, J. Trull, R. Vilaseca, K. Staliunas, W. Krolikowski, S. M. Saltiel, and Y. Kivshar, Opt. Express **17**, 20117 (2009).
[19]C. D. Chen, J. Lu, Y. H. Liu, X. P. Hu, L. N. Zhao, Y. Zhang, G. Zhao, Y. Yuan, and S. N. Zhu, Opt. Lett. **36**, 1227 (2011).
[20]Y. Sheng, W. J. Wang, R. Shiloh, V. Roppo, Y. F. Kong, A. Arie, and W. Krolikowski, Appl. Phys. Lett. **98**, 241114 (2011).
[21]Y. Sheng, W. J. Wang, R. Shiloh, V. Roppo, A. Arie, and W. Krolikowski, Opt. Lett. **36**, 3266 (2011).